

## Current-injection spiral-shaped microcavity disk laser diodes with unidirectional emission

M. Kneissl,<sup>a)</sup> M. Teepe, N. Miyashita, and N. M. Johnson  
Palo Alto Research Center Inc. (PARC), Palo Alto, California 94304

G. D. Chern and R. K. Chang  
Department of Applied Physics, Yale University, New Haven, Connecticut 06520

(Received 11 December 2003; accepted 4 February 2004)

A spiral-shaped microcavity heterojunction laser diode fabricated with InGaN multiple quantum wells is demonstrated to operate under current injection conditions and emit unidirectionally. Room-temperature laser operation was achieved for microcavity disk radii ranging from 50 to 350  $\mu\text{m}$  and threshold current densities as low as 4.6 kA/cm<sup>2</sup>. Unidirectional laser emission is clearly revealed in the far-field pattern with the lateral divergence angle ranging from 60° to 75°. Output power of more than 25 mW was obtained for emission wavelengths near 400 nm. © 2004 American Institute of Physics. [DOI: 10.1063/1.1691494]

Laser emission from microresonator structures, such as microdisks, microcylinders, and microspheres, has been intensely pursued for more than a decade<sup>1–4</sup> because of the extremely high  $Q$  factors<sup>5</sup> and very low threshold power densities<sup>6</sup> that can be achieved in such structures. These features make microresonator lasers attractive candidates for a number of applications, including fiber communication, optical storage, and chemical and biological sensing. In addition, one of the critical impediments to any real-world application of these devices—namely, efficient extraction of light circulating within the microresonator—has recently been overcome with our introduction of a spiral-shaped microresonator structure that was shown to produce unidirectional laser emission under optical pumping conditions.<sup>7</sup> In this letter, we report an important development of practical microresonator lasers with operation of a spiral microcavity disk laser diode under current injection conditions.

Microresonator lasers emit from so-called whispering gallery modes (WGMs), which circulate around the perimeter of the cavity and are confined by total internal reflection at the dielectric interface of the resonator sidewalls. Due to the high degree of symmetry inherent in the simple geometric shapes (e.g., disks, cylinders, and spheres), the laser emission tends to be spatially distributed and therefore difficult to efficiently extract and collect for practical purposes. A number of alternative resonator designs have been proposed in order to localize the output of microcavity lasers into narrowly defined directions. One of these approaches utilizes the evanescent wave coupling of the WGM into closely spaced linear waveguides.<sup>6,8</sup> This approach, however, requires very accurate control of the spacing between the microresonator and the adjacent waveguide. Another alternative design utilizes so-called asymmetric resonant cavity (ARC) lasers. In an ARC structure, the smooth deformation from the normally circular symmetry of the resonator cavity enhances the light outcoupling from distorted WGMs or librational modes, such as “bow-tie” modes.<sup>9,10</sup> However, inherent to its high symmetry, ARC lasers still emit in several directions

and exhibit far-field patterns with multiple lobes. This difficulty has been overcome with the introduction of spiral-shaped microcavity structures that provide unidirectional laser emission, as further described subsequently.

The InGaAlN heterostructure was grown by metalorganic chemical vapor deposition (MOCVD) on (0001) sapphire substrates.<sup>11,12</sup> After the deposition of a low-temperature GaN nucleation layer, a 4- $\mu\text{m}$ -thick Si-doped GaN current-spreading layer was grown, followed by a 50-nm-thick Si-doped In<sub>0.02</sub>Ga<sub>0.98</sub>N layer and a 1- $\mu\text{m}$ -thick Si-doped Al<sub>0.08</sub>Ga<sub>0.92</sub>N cladding layer. The active region of the device is comprised of five 35-Å-thick In<sub>0.1</sub>Ga<sub>0.9</sub>N quantum wells separated by 65-Å-thick GaN barriers and capped with a 20-nm-thick Mg-doped Al<sub>0.2</sub>Ga<sub>0.8</sub>N electron confinement layer. Si- and Mg-doped GaN waveguides, each 100 nm thick and a 500-nm-thick Mg-doped Al<sub>0.08</sub>Ga<sub>0.92</sub>N cladding layer, providing transverse optical mode confinement surround the active region. The laser heterostructure was completed with a 20-nm-thick Mg-doped GaN contact layer grown on top of the  $p$ -AlGaIn cladding layer.

After MOCVD growth the laser heterostructures were

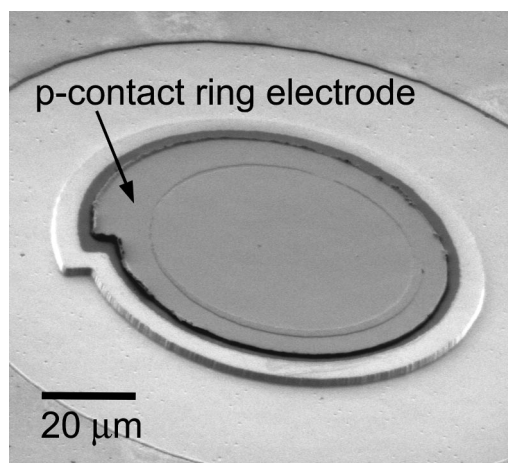


FIG. 1. SEM image of a microcavity disk laser diode with a disk radius of 50  $\mu\text{m}$ . The  $p$ -contact ring electrode defines the areas through which carriers are injected into the microdisk and where stimulated emission can take place.

<sup>a)</sup>Electronic mail: kneissl@parc.com

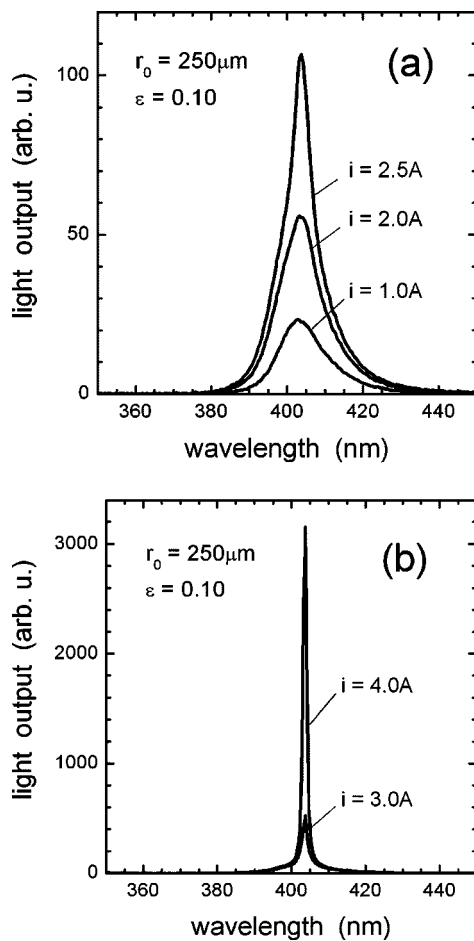


FIG. 2. (a) RT emission spectra of a spiral-shaped InGaN multiple quantum well microcavity disk laser diode measured below threshold with forward bias ranging between 1.0 and 2.5 A. The measurements were performed under pulsed current-injection conditions with a pulse width of 100 ns and a repetition frequency of 1 kHz. The radius of the spiral microdisk was  $r_0=250\ \mu\text{m}$  and the deformation parameter  $\epsilon=0.10$ . (b) RT emission spectra for the same laser diode measured above threshold for drive currents of 3.0 and 4.0 A, respectively.

etched into spiral cross sections by chemically assisted ion-beam etching<sup>12</sup> with disk radii  $r_0$  ranging between 50 and  $350\ \mu\text{m}$ . The basic configuration of a spiral-shaped microcavity disk laser diode is shown in the scanning electron microscope (SEM) micrograph of Fig. 1. The spiral cross section is defined by  $r(\Phi)=r_0(1+\epsilon\Phi/2\pi)$ , where  $\epsilon$  is the deformation parameter and  $r_0$  is the radius at  $\Phi=0$ . The angularly varying cross-sectional radius creates a “notch” at the perimeter of the spiral micro-disk at  $\Phi=2\pi$ , as shown in Fig. 1 and in the inset of Fig. 4. The spiral-shaped design results in efficient out-coupling of the light from the laser resonator through diffraction of the whispering gallery modes at the notch and also provides unidirectional emission.<sup>7</sup> The  $p$ -contact ring electrode defines the area into which carriers are injected in the microdisk and where optical gain is generated. The outer edge of the  $p$ -electrode follows closely the perimeter of the microdisk sidewall, and the width of the  $p$ -electrode was chosen to have adequate overlap with the WGMs in the resonator structure.

Laser emission from an electrically driven spiral microcavity disk laser diode is demonstrated in Figs. 2(a) and 2(b) with a series of emission spectra recorded at different current injection levels below and above threshold. The spectra were

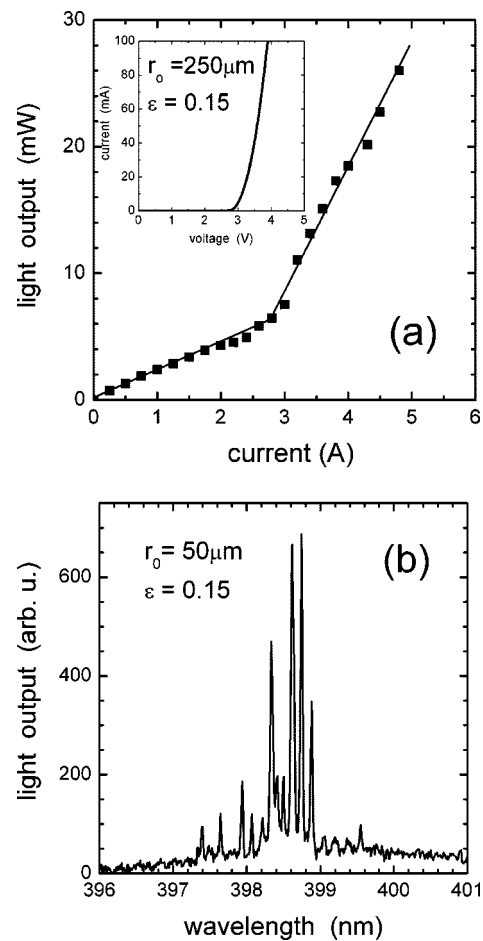


FIG. 3. (a) RT  $L-I$  characteristic for a spiral-shaped microdisk laser diode (500 ns pulse width, repetition frequency 1 kHz). The radius of the spiral microdisk was  $r_0=250\ \mu\text{m}$  and the deformation parameter  $\epsilon=0.15$ . A change in the slope of the  $L-I$  characteristics is observed near 3.1 A, corresponding to a threshold current density of  $7.8\ \text{kA}/\text{cm}^2$ . The squares are measured data points; the line is a guide for the eye. The inset shows the  $V-I$  characteristic for the same device. (b) High-resolution emission spectrum of a spiral microcavity disk laser diode with a radius of  $r_0=50\ \mu\text{m}$  ( $\epsilon=0.15$ ) recorded above threshold. The measured mode spacing is about 0.13 nm, and the spectral FWHM is less than 0.04 nm.

measured at RT under pulsed current conditions (100 ns pulse width, 1 kHz repetition frequency) on microcavity disks with a radius of  $250\ \mu\text{m}$  and  $\epsilon=0.10$ . Figure 2(a) shows relatively broad spontaneous emission measured below threshold, with the emission peak near 404 nm and a full width at half-maximum (FWHM) of 14 nm. With the onset of laser operation at a pulsed current of 3.0 A, a sudden narrowing of the (stimulated) emission spectrum can be observed with a measured FWHM of 1.3 nm, which was the resolution limit of the spectrometer. Above threshold, the laser light is strongly TE polarized, with a TE/TM polarization ratio greater than 200.

Further evidence of lasing under current injection is provided in Figs. 3(a) and 3(b). Figure 3(a) shows the RT pulsed light-output versus current ( $L-I$ ) characteristic for a spiral microdisk laser diode with  $r_0=250\ \mu\text{m}$  and  $\epsilon=0.15$ . The inset in Fig. 3(a) shows the voltage versus current ( $V-I$ ) characteristic for the same device. At the onset of lasing at a forward current of 3.1 A, a change in the slope of the  $L-I$  characteristics is clearly observed. The measured threshold current corresponds to a threshold current density of  $7.8$

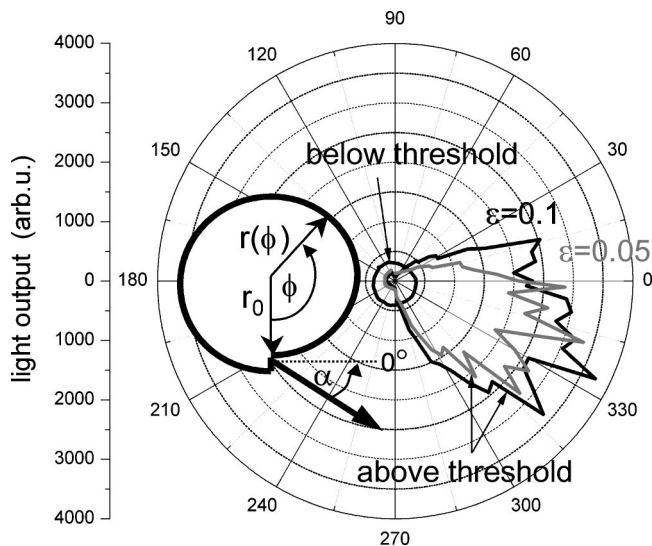


FIG. 4. Radial distribution of the light output from the spiral-shaped microdisk laser diode measured below and above threshold. The radius of the spiral microdisk was  $r_0=250 \mu\text{m}$  and the deformation parameters were  $\epsilon=0.05$  (gray) and  $\epsilon=0.10$  (black). An emission beam at angle of  $\alpha=0^\circ$  corresponds to a direction normal to the notch surface as shown in the inset. Below laser threshold, the emission pattern is essentially isotropic and independent of the deformation parameter. Above threshold, directional emission is clearly observed with the emission direction at a tilt angle  $\alpha \sim 25^\circ$ . The measured divergence angle of the far-field pattern is  $\sim 75^\circ$  for  $\epsilon=0.10$  and  $\sim 60^\circ$  for  $\epsilon=0.05$ .

$\text{kA}/\text{cm}^2$  and a maximum output power of 26 mW. Even lower threshold current densities of  $4.6 \text{ kA}/\text{cm}^2$  were achieved for devices with disk radii of  $r_0=350 \mu\text{m}$ . Figure 3(b) shows a high-resolution emission spectrum for a microdisk laser diode with a radius of only  $r_0=50 \mu\text{m}$  and a deformation parameter of  $\epsilon=0.15$ . The RT spectrum was recorded above threshold at a pulsed current of 6.1 A. Due to the small diameter of the microdisk, it is possible to resolve multiple radial modes in the spectrum with an average mode spacing of  $\Delta\lambda \sim 0.13 \text{ nm}$ . The observations are in good agreement with the expected mode spacing, which is related to the disk radius as follows:<sup>13</sup>

$$r = \frac{\lambda_0^2}{2\pi\Delta\lambda \left( n_{\text{eff}} - \lambda_0 \frac{dn}{d\lambda} \right)},$$

where  $r$  is the effective radius of the microdisk,  $\lambda_0$  is the laser wavelength in the cavity,  $n_{\text{eff}}$  is the effective refractive index for the transverse optical mode, and  $dn/d\lambda$  is the first-order dispersion in GaN. For a refractive index of  $n=2.6$ , a dispersion term  $\lambda_0 dn/d\lambda = -1.6$  (Ref. 14), and  $\lambda_0=399 \text{ nm}$ , the radius extracted from the measured mode spacing is  $r=45 \mu\text{m}$ , which is consistent with the expectation that the modes should have the highest intensity close to the perimeter of the disk.

Unidirectional laser emission under current injection conditions is demonstrated in Fig. 4 with radial distributions of the light output measured below and above threshold. The radius of the spiral microdisk was  $r_0=250 \mu\text{m}$  and the deformation parameters were  $\epsilon=0.05$  (gray) and  $\epsilon=0.10$  (black). Emission directed towards an angle of  $0^\circ$  corresponds to an output beam normal to the notch surface. Below laser threshold, the spontaneous emission pattern is essen-

tially isotropic and independent of the deformation parameter. Above threshold, directional emission can be clearly observed with the peak laser emission tilted at an angle of about  $-25^\circ$  away from the surface normal of notch. This tilt in the emission beam is somewhat counterintuitive since one would expect from a simple ray picture that the beam should escape in a direction that is basically surface normal to the notch. However, detailed calculations of the electric field in the microdisk show that the resonance in the spiral exhibits a strong chirality.<sup>7</sup> It was found that clockwise waves are diffracted at the notch and coupled into counterclockwise (ccw) modes, which are then responsible for the efficient outcoupling of the light from the disk. The tilt in the escape angle is a result of the spread in wave vectors from the different ccw modes.<sup>7</sup> The calculated far-field profile agrees reasonably well with the observed tilt in the emission beam angle and the measured lateral divergence angle of the far-field pattern of  $\sim 75^\circ$  for the microdisk with  $\epsilon=0.10$  and  $\sim 60^\circ$  for a disk with  $\epsilon=0.05$ .

Taken together, the device performance documented in Figs. 2–4 provides compelling evidence for the achievement of laser operation with unidirectional emission under current injection in a spiral-shaped microcavity disk laser diode. These microresonator devices constitute a particular class of laser diodes that combines some of the best features from both edge-emitting and vertical-cavity surface-emitting laser diodes, such as high-power operation, wafer-level testing, and the ability to fabricate arrays of diodes or to integrate them with other optoelectronic components. The attainment of a practical microcavity laser diode configuration, with current injection and unidirectional emission, opens the way for exploration of applications uniquely suited to these capabilities.

This work was supported in part by NSF, AFOSR, and the Defense Advanced Research Projects Agency SUVOS program under SPAWAR Systems Center Contract No. N66001-02-C-8017 monitored by LTC Dr. J. Carrano.

<sup>1</sup>S.-X. Qian, J. B. Snow, H.-M. Tzeng, and R. K. Chang, *Science* **231**, 486 (1986).

<sup>2</sup>S. L. McCall, A. F. J. Levi, R. E. Slusher, S. J. Pearton, and R. A. Logan, *Appl. Phys. Lett.* **60**, 289 (1991).

<sup>3</sup>A. F. J. Levi, R. E. Slusher, S. L. McCall, S. J. Pearton, and W. S. Hobson, *Appl. Phys. Lett.* **62**, 2021 (1993).

<sup>4</sup>Y. Yamamoto and E. Slusher, *Phys. Today* **46**, 66 (1993).

<sup>5</sup>D. K. Armani, T. J. Kippenberg, S. M. Spillane, and K. J. Vahala, *Nature (London)* **421**, 925 (2003).

<sup>6</sup>S. M. Spillane, T. J. Kippenberg, and K. J. Vahala, *Nature (London)* **415**, 621 (2002).

<sup>7</sup>G. D. Chern, H. E. Tureci, A. D. Stone, M. Kneissl, N. M. Johnson, and R. K. Chang, *Appl. Phys. Lett.* **83**, 1710 (2003).

<sup>8</sup>R. K. Chang and A. J. Campillo, *Optical Processes in Microcavities* (World Scientific, Singapore, 1996), Chap. 10.

<sup>9</sup>J. U. Nöckel and A. D. Stone, *Nature (London)* **385**, 45 (1997).

<sup>10</sup>C. Gmachl, F. Capasso, E. E. Narimanov, J. U. Nöckel, A. D. Stone, J. Faist, D. L. Sivco, and A. Y. Cho, *Science* **280**, 1556 (1998).

<sup>11</sup>M. Kneissl, D. P. Bour, L. T. Romano, C. G. Van de Walle, J. E. Northrup, W. S. Wong, D. W. Treat, M. Teepe, T. Schmidt, and N. M. Johnson, *Appl. Phys. Lett.* **77**, 1931 (2000).

<sup>12</sup>M. Kneissl, D. P. Bour, N. M. Johnson, L. T. Romano, B. S. Krusor, R. Donaldson, J. Walker, and C. Dunnrowicz, *Appl. Phys. Lett.* **72**, 1539 (1998).

<sup>13</sup>S. Chang, N. B. Rex, R. K. Chang, G. Chong, and L. J. Guido, *Appl. Phys. Lett.* **75**, 166 (1999).

<sup>14</sup>E. Ejder, *Phys. Status Solidi A* **6**, 445 (1971).